Supporting Information for:

Selective Anion Binding by a "Chameleon" Capsule with a Dynamically Reconfigurable Exterior

Yana R. Hristova, Maarten M. J. Smulders, Jack K. Clegg, Boris Breiner and Jonathan R. Nitschke*

University of Cambridge, Department of Chemistry
Lensfield Road, Cambridge CB2 1EW, United Kingdom
E-mail: jrn34@cam.ac.uk
Homepage: http://www-jrn.ch.cam.ac.uk/

Table of Contents:

1. Experimental

All reagents and solvents were purchased from commercial sources and used as supplied. NMR spectra were recorded on a Bruker Avance DPX400 spectrometer; δ_H values are reported relative to acetonitrile-d_3 at 1.94 ppm. Low resolution electrospray ionisation mass spectra (ESI-MS) were obtained on a Micromass Quattro LC, infused from a Harvard Syringe Pump at a rate of 10 μL per minute. Mass spectra provided by the EPSRC National MS Service Centre at Swansea were acquired on a Thermofisher LTQ Orbitrap XL. FT-IR spectra were collected using a Perkin Elmer Spectrum 100 FT-IR spectrometer.

1.1. Synthesis and Characterisation

3,3′-bipyridine-6,6′-dicarboxaldehyde:[S1] A solution of 6,6′-dimethyl-3,3′-bipyridine (this precursor was synthesised following a previously reported literature procedure)[S2] (1.00 g, 5.43 mmol) in degassed DMSO (40 mL) was prepared in a round-bottom flask. Iodine (2.75 g, 10.86 mmol) was added and the solution was stirred for 10 minutes under nitrogen. Trifluoroacetic acid (1.17 mL, 15.20 mmol) was added drop wise *via* a syringe. The reaction was refluxed for three hours at 150 °C under nitrogen. After cooling to room temperature, the reaction was quenched with a 14% aqueous sodium thiosulfate solution and further diluted with a saturated sodium bicarbonate solution. The product was extracted with dichloromethane (3×20 mL), the yellow organic layer was washed with water and dried over $MgSO_4$. After filtration, the solvent was evaporated and the remaining solid was washed thoroughly with Et_2O several times. The product 3,3′-bipyridine-6,6′-dicarboxaldehyde was obtained as a beige fine powder (0.337 g, 29% yield).

^{1}H NMR (400 MHz, 298 K, CD_3CN): δ = 10.09 (s, 2H, aldehyde), 9.16 (s, 2H, pyridine), 8.31 (d, J = 8.03 Hz, 2H, pyridine), 8.07 (d, J = 8.03 Hz, 2H, pyridine); ^{13}C NMR (400 MHz, 298 K, $CDCl_3$): δ = 191.0, 151.1, 147.1, 134.7, 134.1, 120.3; Elemental Analysis (%) calcd for $C_{12}H_8N_2O_2$•0.35CH_2Cl_2: C 61.31, H 3.62, N 11.58; found: C 61.26, H 3.67, N 11.73. FT-IR: ν (cm^{-1}): 2851(br), 1704, 1581, 1560, 1344, 1303, 1274, 1202, 999, 844, 824, 738, 676.

Preparation of [1](NTf$_2$)$_8$: 3,3′-bipyridine-6,6′-dicarboxaldehyde (38.2 mg, 0.18 mmol), aniline (32.9 μL, 0.36 mmol), and iron(II) trifluoromethanesulfonimide dihydrate (78.8 mg, 0.12 mmol) were added to a 25 mL Schlenk flask containing degassed acetonitrile (6 mL). The flask was sealed and subjected to three evacuation/nitrogen fill cycles. The reaction was stirred for 24 hours at 323 K. [**1**](NTf$_2$)$_8$ was precipitated as a purple powder by the addition of diisopropyl ether (yield 110 mg, 79%); ^{1}H NMR (400 MHz, 298 K, CD$_3$CN): δ = 9.05 (s, 12H, imine), 8.65 (d, *J* = 8.4 Hz, 12H, 5,5′-bipyridine), 8.36 (d, *J* = 8.0 Hz, 12H, 6,6′-bipyridine), 7.48 (t, *J* = 7.7 Hz, 12H, 4-aniline), 7.27 (t, *J* = 8.0 Hz, 24H, 3-aniline), 7.09 (s, 12H, 2,2′-bipyridine), 5.44 ppm (d, *J* = 7.7 Hz, 24H, 2-aniline); ^{13}C NMR (400 MHz, 298 K, CD$_3$CN): δ = 178.5, 176.0, 160.8 (1,4-difluorobenzene as internal standard), 159.9, 158.9 (1,4-difluorobenzene as internal standard), 152.9, 150.7, 142.9, 138.9, 131.3, 130.8, 130.4, 122.1 (triflimide anion); Elemental Analysis (%) calcd for C$_{160}$H$_{108}$F$_{48}$Fe$_4$N$_{32}$O$_{32}$S$_{16}$·5H$_2$O: C 40.63, H 2.52, N 9.48; found: C 40.65, H 2.52, N 9.20; ESI-MS: *m/z*: 2039.1 ({[**1**](NTf$_2$)$_6$}$^{2+}$), 1266.2 ({[**1**](NTf$_2$)$_5$}$^{3+}$), 879.1 ({[**1**](NTf$_2$)$_4$}$^{4+}$ and {[Fe$_2$L$_3$](NTf$_2$)$_2$}$^{2+}$), 492.7 ({[Fe$_2$L$_3$](NTf$_2$)}$^{3+}$), 299.8 ([Fe$_2$L$_3$]$^{4+}$). Purple-plate like crystals of [MeCN⊂**1**]·8NTf$_2$·MeCN suitable for X-ray diffraction studies were grown from the slow diffusion of toluene into an acetonitrile solution of [**1**](NTf$_2$)$_8$ over several days and were used directly in analysis. For X-ray analysis, see Section 2.

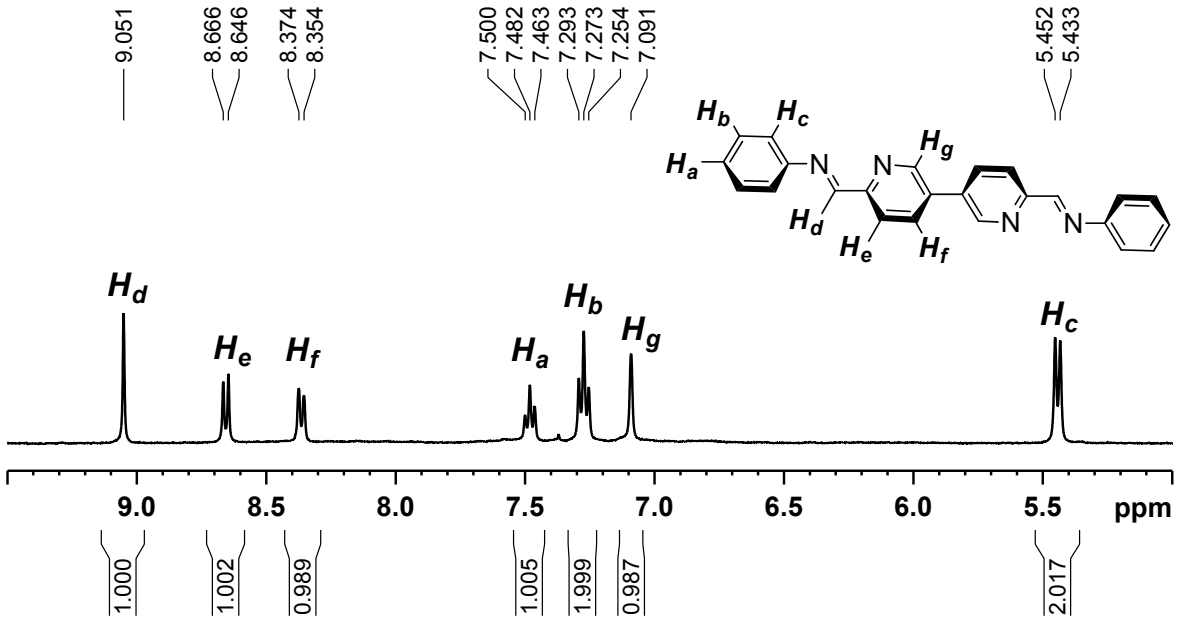

Figure S1: ^{1}H NMR spectrum of **1** (CD$_3$CN, 400 MHz, 298 K); only aromatic region shown for clarity.

Synthesis of [2](BF$_4$)$_8$: Into a Schlenk flask 3,3′-bipyridine-6,6′-dicarboxaldehyde (29.60 mg, 0.140 mmol), *p*-chloroaniline (36.10 mg, 0.283 mmol), and Fe(BF$_4$)$_2$•6H$_2$O (33.40 mg, 0.100 mmol) were dissolved in 8 mL of acetonitrile. The flask was sealed and the solution was purified of dioxygen by three vacuum/nitrogen fill cycles. The solution was sonicated for 10 minutes and was heated at 323 K for one day. After cooling to room temperature, the solution was layered with *i*-Pr$_2$O and was left undisturbed for a few days. The dark-purple precipitation was isolated and dried to give 62.14 mg of **2** (76% yield).

^{1}H NMR (400 MHz, 298 K, CD$_3$CN): δ = 9.21 (s, 2H, imine), 8.60 (d, *J* = 8.60 Hz, 2H, pyridine), 8.21 (d, *J* = 8.30 Hz, 2H, pyridine), 7.32 (d, *J* = 8.56 Hz, 4H, aniline), 7.31 (s, 2H, pyridine), 5.61 (d, *J* = 8.56 Hz, 4H, aniline). ESI-MS: *m/z*: 614.2 [**2**+3BF$_4^-$]$^{5+}$, 789.6 [**2**+4BF$_4^-$]$^{4+}$, 1081.7 [**2**+5BF$_4^-$]$^{3+}$.

Synthesis of [3](BF$_4$)$_8$: Into a Schlenk flask 3,3′-bipyridine-6,6′-dicarboxaldehyde (29.25 mg, 0.138 mmol), *p*-toluidine (30.86 mg, 0.288 mmol), and Fe(BF$_4$)$_2$•6H$_2$O (31.50 mg, 0.093 mmol) were dissolved in 8 mL of acetonitrile. The flask was sealed and the solution was purified of dioxygen by three vacuum/nitrogen fill cycles. The solution was sonicated for 10 minutes and was heated at 323 K for one day. After cooling to room temperature, the solution was layered with *i*-Pr$_2$O and was left undisturbed for a few days. The dark-purple precipitation was isolated and dried to give 71.51 mg of **3** (95% yield).

^{1}H NMR (400 MHz, 298 K, CD$_3$CN): δ = 9.00 (s, 2H, imine), 8.52 (d, *J* = 8.03 Hz, 2H, pyridine), 8.19 (d, *J* = 7.78 Hz, 2H, pyridine), 7.26 (s, 2H, pyridine), 7.03 (d, *J* = 7.78 Hz, 4H, aniline), 5.42 (d, *J* = 7.78 Hz, 4H, aniline), 2.34 (s, 3H, methyl). ESI-MS: *m/z*: 565.4 [**3**+3BF$_4^-$]$^{5+}$, 728.2 [**3**+4BF$_4^-$]$^{4+}$, 1000.0 [**3**+5BF$_4^-$]$^{3+}$, 1543.4 [**3**+6BF$_4^-$]$^{2+}$.

Synthesis of the library R•5 of Scheme 3: 3,3´-bipyridine-6,6´-dicarboxaldehyde (3.48 mg, 0.0164 mmol, 6 equivalents), *p*-chloroaniline (1.51 mg, 0.0118 mmol, 4.3 equivalents), *p*-bromoaniline (1.96 mg, 0.0114 mmol, 4.2 equivalents), *p*-iodoaniline (2.45 mg, 0.0112 mmol, 4.1 equivalents), and iron(II) trifluoromethanesulfonate (3.90 mg, 0.0110 mmol, 4.0 equivalents) were loaded into a J-Young NMR tube and dissolved in CD_3CN with *t*BuOH as the internal standard (10.6 μL). All starting materials dissolved, giving a dark purple solution. The NMR tube was sealed, and the atmosphere was purified of dioxygen by three evacuation/nitrogen fill cycles. The reaction was heated for 2 days at 323 K; the resulting product mixture was then characterised by ^{1}H NMR and ESI-MS.

^{1}H NMR (400 MHz, 298 K, CD_3CN): δ = 9.34 (m, 2H, imine), 8.69 (br. d, 2H, pyridine), 8.30 (br. d, 2H, pyridine), 7.64, 7.45, 7.30 (three doublets, *J* = 7.0 Hz, 4H, aniline), 7.36 (d, *J* = 8.2 Hz, 2H, free *p*-iodoaniline), 7.19 (overlapping signals: s, 2H, pyridine; d, 2H, free *p*-bromoaniline), 7.07 (d, *J* = 8.2 Hz, 2H, free *p*-chloroaniline), 6.65 (d, *J* = 8.2 Hz, 2H, free *p*-chloroaniline), 6.59 (d, *J* = 8.3 Hz, 2H, free *p*-bromoaniline), 6.49 (d, *J* = 8.1 Hz, 2H, free *p*-iodoaniline), 5.64 – 5.37 (three multiplets, 4H, aniline); for ESI-MS data and assignment, see Fig. S2.

To the same tube, *p*-methoxyaniline (4.08 mg, 0.0331 mmol, 12.1 equivalents) was added and the reaction was heated for one more day, resulting in the formation of **4** and the release of all halogenated anilines.

^{1}H NMR (400 MHz, 298 K, CD_3CN): δ = 9.26 (s, 2H, imine), 8.62 (d, *J* = 7.9 Hz, 2H, pyridine), 8.22 (d, *J* = 7.6 Hz, 2H, pyridine), 7.35 (d, *J* = 8.0 Hz, 2H, free *p*-iodoaniline), 7.18 (overlapping signals: s, 2H, pyridine; d, 2H, free *p*-bromoaniline), 7.05 (d, *J* = 8.0 Hz, 2H, free *p*-chloroaniline), 6.78 (d, *J* = 8.2 Hz, 4H, aniline), 6.71 (d, *J* = 8.0 Hz, 2H, free *p*-methoxyaniline), 6.64 – 6.55 (m, 2H for each free *p*-methoxy-, *p*-chloro-, *p*-bromo-, and *p*-iodoaniline), 5.72 (d, *J* = 8.2 Hz, 4H, aniline), 3.79 (s, 3H, incorporated MeO), 3.68 (s, 3H, free MeO). ESI-MS: *m/z*: 640.7 [**4**+3OTf$^-$]$^{5+}$, 838.2 [**4**+4OTf$^-$]$^{4+}$, 1167.2 [**4**+5OTf$^-$]$^{3+}$, 1825.2 [**4**+6OTf$^-$]$^{2+}$.

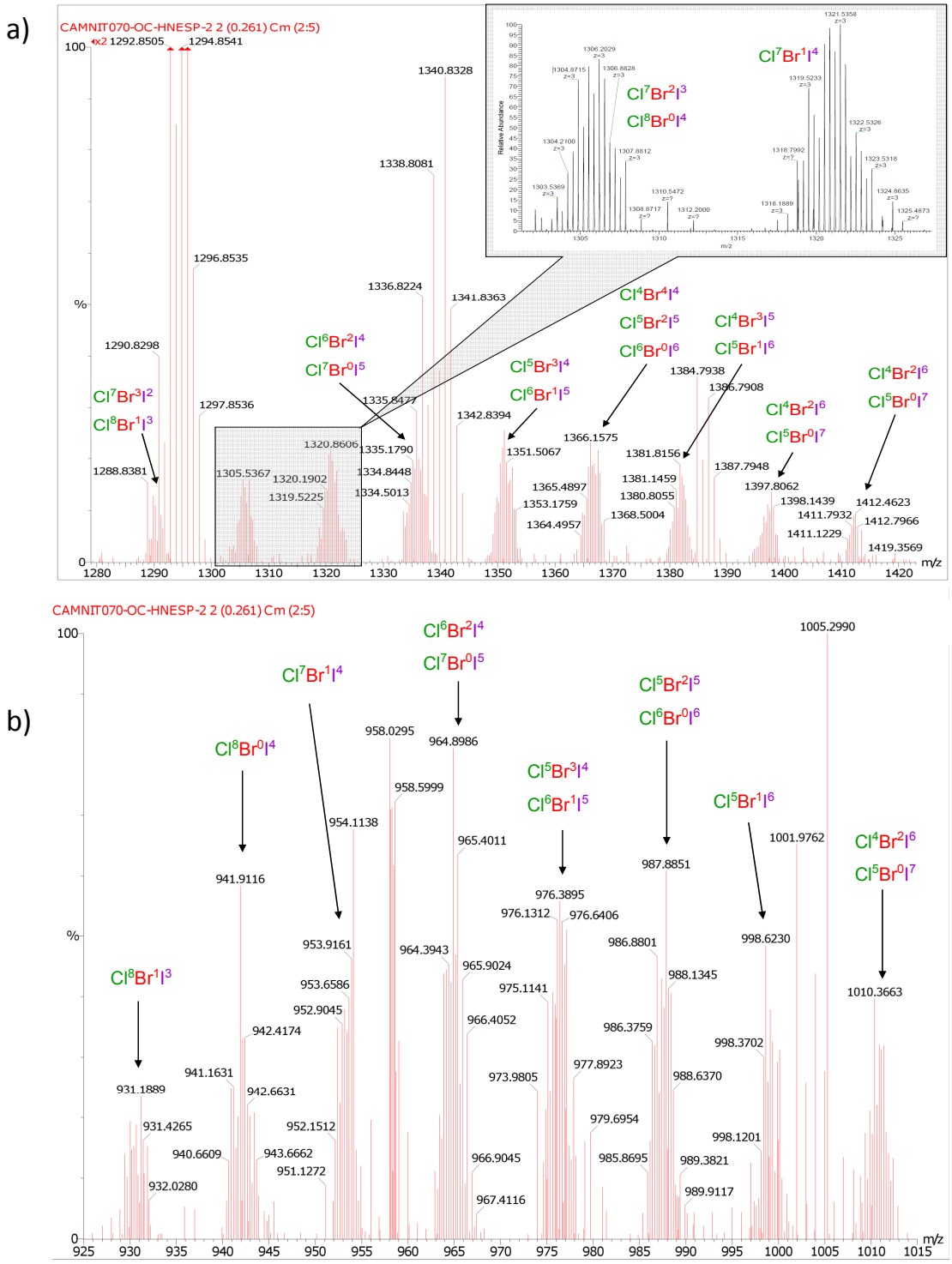

Figure S2: ESI-MS of library **R•5** (where **R** = $Cl^{x}Br^{y}I^{z}$ and $x + y + z = 12$): a) +3 clusters; b) +4 clusters.

1.1.1. Aniline Subcomponent Substitution

2→3: Into a J-Young NMR tube **2** (4.90 mg, 0.0017 mmol, 1 eq.), *p*-toluidine (2.69 mg, 0.025 mmol, 14.7 eq.) and CD_3CN (0.5 mL) were added. The tube was sealed and the solution was purified of dioxygen by three vacuum/nitrogen fill cycles. The dark purple solution was sonicated and heated at 323 K for one day.

^{1}H NMR (400 MHz, 298 K, CD_3CN): δ = 9.01 (s, 2H, imine), 8.54 (d, *J* = 7.64 Hz, 2H, pyridine), 8.22 (d, *J* = 7.41 Hz, 2H, pyridine), 7.25 (s, 2H, pyridine), 7.05 (brs, 2H, free *p*-chloroaniline), 6.94 (brs, 4H, *p*-toluidine), 6.59 (brs, 2H, free *p*-chloroaniline), 5.43 (d, *J* = 7.56 Hz, 4H, *p*-toluidine), 2.34 (s, 3H, methyl). ESI-MS: *m/z*: 565.2 $[\mathbf{3}+3BF_4^-]^{5+}$, 728.3 $[\mathbf{3}+4BF_4^-]^{4+}$, 1000.1 $[\mathbf{3}+5BF_4^-]^{3+}$.

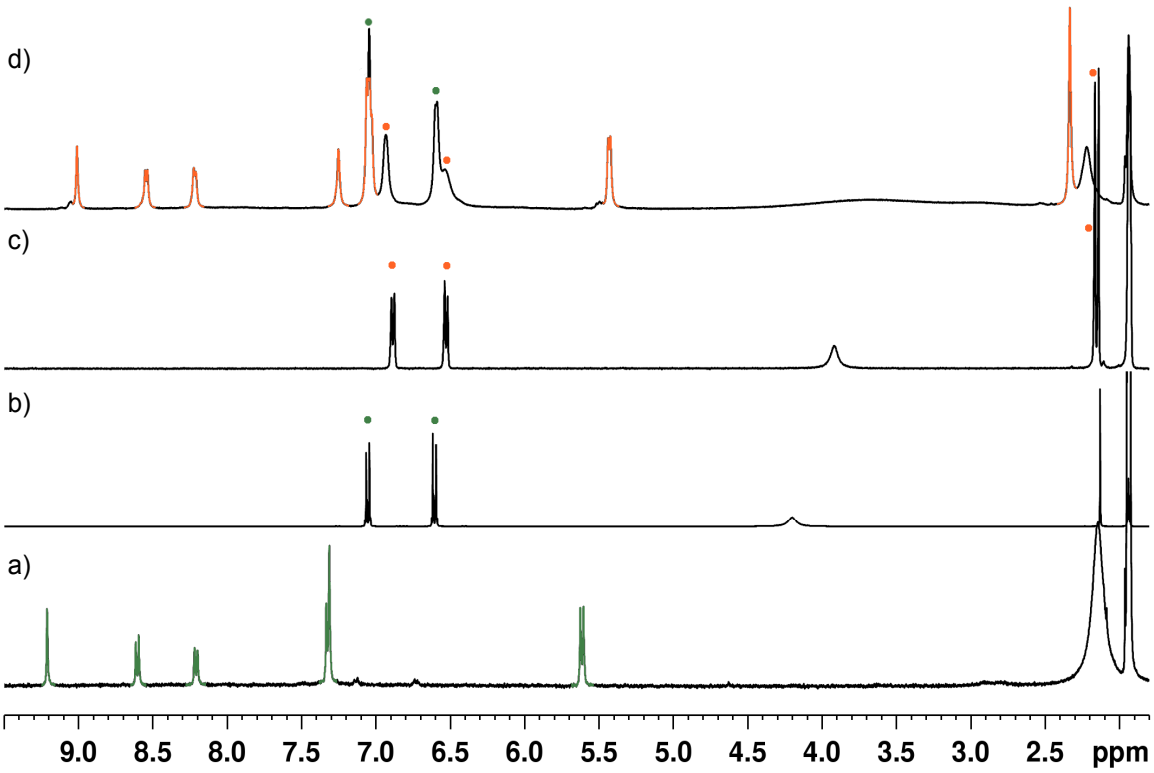

Figure S3: ^{1}H NMR of the transformation of **2→3**: a) **2** prepared from subcomponents; b) *p*-chloroaniline; c) *p*-toluidine; d) substitution reaction of **2→3** (CD_3CN, 400 MHz, 298 K).

2→4: Into a J-Young NMR tube **2** (3.25 mg, 0.0012 mmol, 1 eq.), *p*-methoxyaniline (1.84 mg, 0.015 mmol, 12.5 eq.) and CD_3CN (0.5 mL) were added. The tube was sealed and the solution was purified of dioxygen by three vacuum/nitrogen fill cycles. The dark purple solution was sonicated and heated at 323 K for one day.

^{1}H NMR (400 MHz, 298 K, CD_3CN): δ = 9.06 (s, 2H, imine), 8.53 (d, *J* = 8.01 Hz, 2H, pyridine), 8.19 (d, *J* = 7.83 Hz, 2H, pyridine), 7.27 (s, 2H, pyridine), 7.05 (d, *J* = 8.53 Hz, 2H, free *p*-chloroaniline), 6.78 (d, *J* = 8.71 Hz, 4H, *p*-methoxyaniline), 6.60 (d, *J* = 8.36 Hz, 2H, free *p*-chloroaniline), 5.67 (d, *J* = 7.71 Hz, 4H, *p*-methoxyaniline), 3.80 (s, 3H, methoxy).

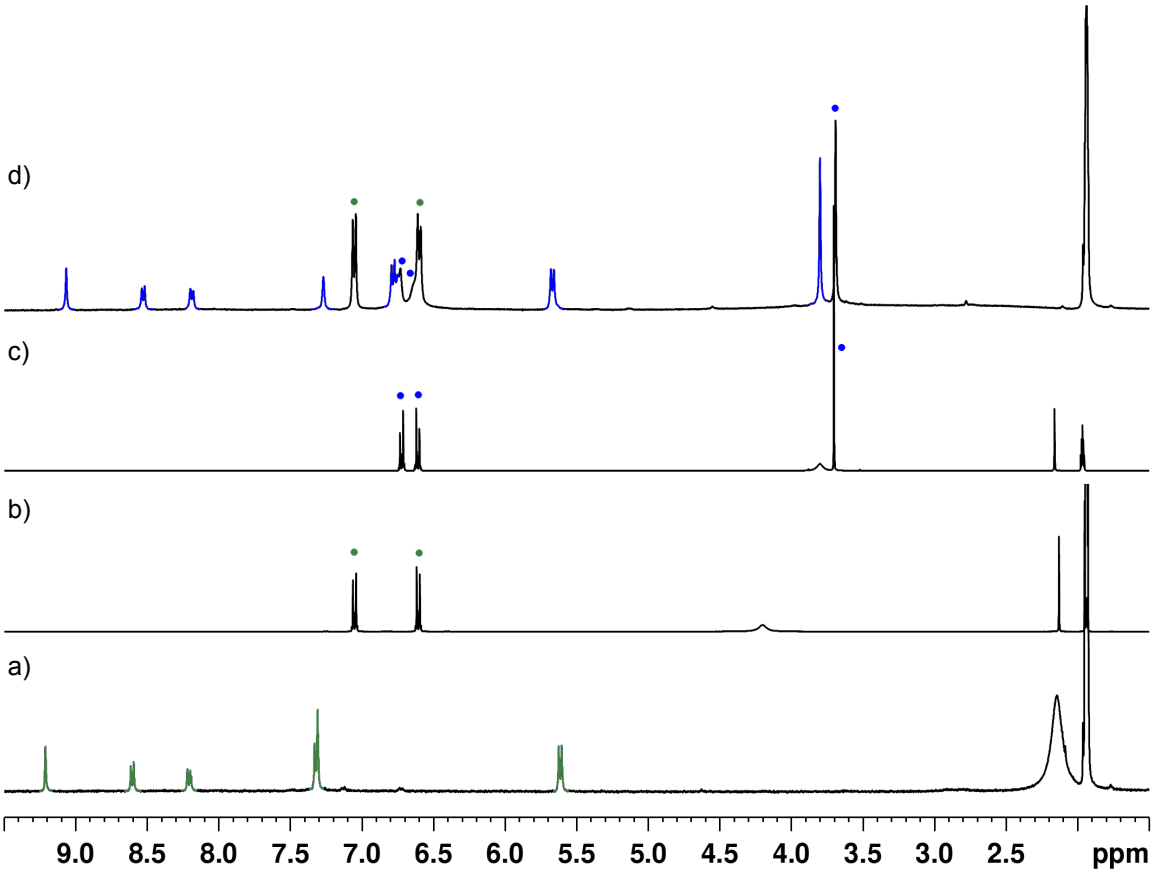

Figure S4: ^{1}H NMR of the transformation of **2→4**: a) **2** prepared from subcomponents; b) *p*-chloroaniline; c) *p*-methoxyaniline; d) substitution reaction of **2→4** (CD_3CN, 400 MHz, 298 K).

3→4: Into a J-Young NMR tube **3** (4.32 mg, 0.0017 mmol, 1 eq.), *p*-methoxyaniline (2.59 mg, 0.021 mmol, 12.5 eq.) and CD_3CN (0.5 mL) were added. The tube was sealed and the solution was purified of dioxygen by three vacuum/nitrogen fill cycles. The dark purple solution was sonicated and heated at 353 K for six days.

^{1}H NMR (400 MHz, 298 K, CD_3CN): δ = 9.07 (s, 2H, imine), 8.53 (d, *J* = 8.36 Hz, 2H, pyridine), 8.19 (d, *J* = 7.66 Hz, 2H, pyridine), 7.27 (s, 2H, pyridine), 6.90 (d, *J* = 7.84 Hz, 2H, free *p*-toluidine), 6.78 (d, *J* = 8.19 Hz, 4H, incorporated *p*-methoxyaniline), 6.70 (d, *J* = 8.36 Hz, 2H, free *p*-methoxyaniline), 6.60 (d, *J* = 8.36 Hz, 2H, free *p*-methoxyaniline), 6.54 (d, *J* = 8.01 Hz, 2H, free *p*-toluidine), 5.68 (d, *J* = 8.88 Hz, 4H, incorporated *p*-methoxyaniline), 3.80 (s, 3H, incorporated methyoxy), 3.68 (s, 3H, free methyoxy), 2.34 (s, 3H, incorporated methyl), 2.18 (s, 3H, free methyl). Note: the aromatic protons of incorporated *p*-toluidine were difficult to attribute due to their low intensity and possible superposition. However, the methyl signal for incorporated *p*-toluidine is indicative of incomplete substitution. ESI-MS: a mixture of products with different degrees of substitution ranging from only two *p*-methoxyanilines (forming a partially substituted **3**) to all twelve *p*-methoxyanilines being incorporated (forming **4**) is observed indicated by complicated distribution patterns with *m/z* ranges: 461.7 – 488.7 $[\mathbf{4}+2BF_4^-]^{6+}$ (from 2 to 12 *p*-methoxyanilines being incorporated), 584.5 – 603.7 $[\mathbf{4}+3BF_4^-]^{5+}$ (from 6 to 12 *p*-methoxyanilines being incorporated), 748.4 – 776.4 $[\mathbf{4}+4BF_4^-]^{4+}$ (from 5 to 12 *p*-methoxyanilines being incorporated).

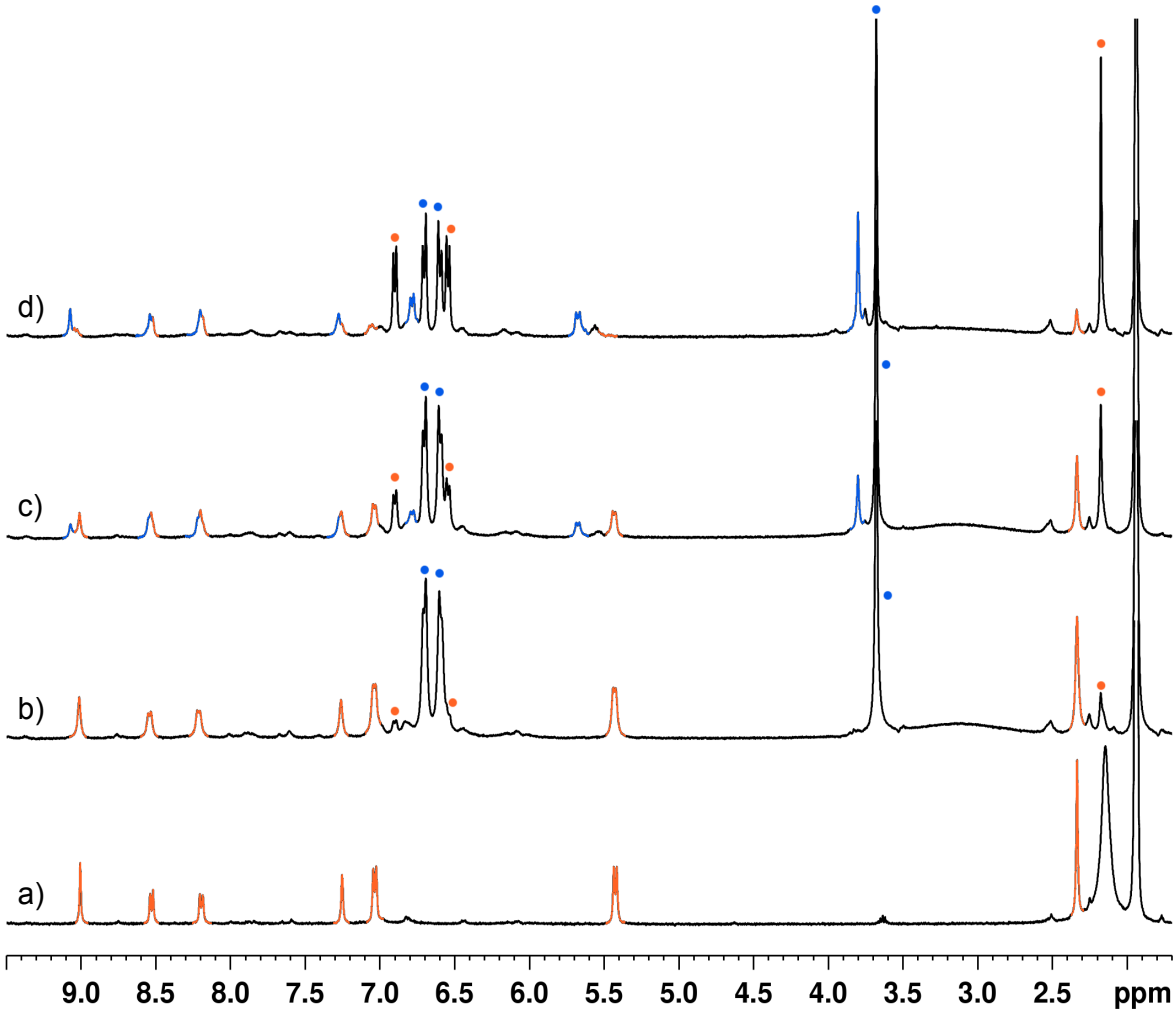

Figure S5: ^{1}H NMR of the transformation of **3**→**4**: a) **3** prepared from subcomponents; b) **3** after addition of 12.5 eq. of *p*-methoxyaniline and 2 hrs of heating at 353 K; c) after 3 days; d) after 6 days at 353 K the substitution reaction has reached equilibrium with 79% of the *p*-toluidine being substituted by *p*-methoxyaniline (orange peaks represent **3**) (CD_3CN, 400 MHz, 298 K).

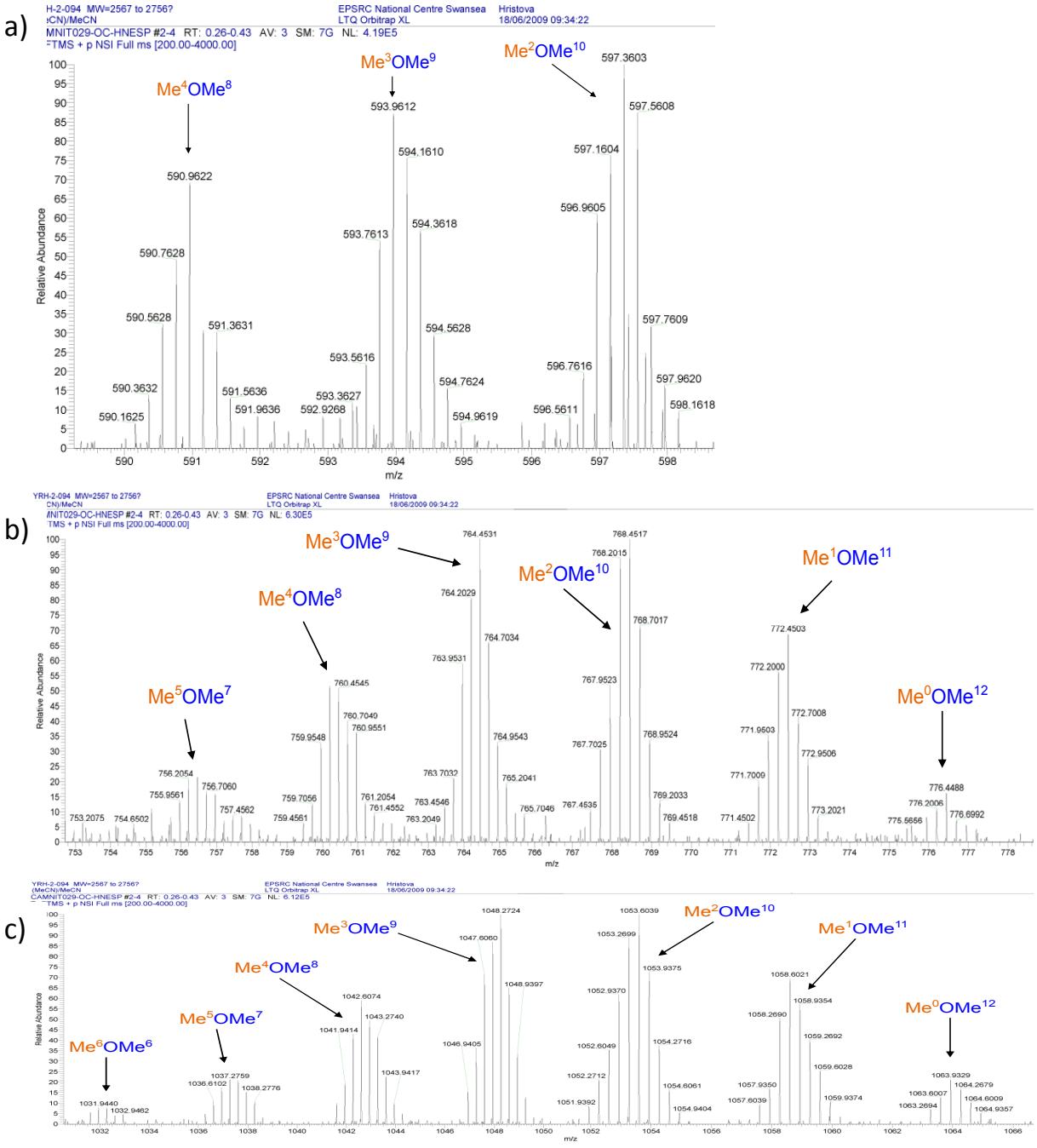

Figure S6: ESI-MS of the transformation of **3**→**4**; a) +5 clusters; b) +4 clusters; c) +3 clusters.

1.1.2. Anion Displacement

Displacement of BF_4^- by PF_6^- within 1: Into a J-Young NMR tube **1** (6.65 mg, 0.0014 mmol, 1 eq.) was dissolved in CD_3CN (0.5 mL) and tetramethylammonium tetrafluoroborate (0.23 mg, 0.0014 mmol, 1 eq., added from a premade stock solution) and 1,4-difluorobenzene (internal standard, 1 μL, 0.010 mmol, 7.32 eq.) were added. The tube was sealed and the solution was purified of dioxygen by three vacuum/nitrogen fill cycles. The dark purple solution was sonicated for 10 minutes and the ^{19}F NMR spectrum shown in Figure S9a was acquired. To the same tube, tetramethylammonium hexafluorophosphate (0.46 mg, 0.0021 mmol, 1.5 eq., added from a premade stock solution in CD_3CN) was added and the ^{19}F NMR spectrum shown in Figure S7b was acquired.

^{19}F NMR (400 MHz, 298 K, CD_3CN): a): δ = –80.3 (s, NTf_2^-), –121.4 (s, 1.4-difluorobenzene), –150.6 (broad s, average of *endo* and *exo* BF_4^-); b): δ = –72.0 (d, J = 717.0 Hz, *endo* PF_6^-), –72.5 (d, J = 707.0 Hz, *exo* PF_6^-) –80.3 (s, NTf_2^-), –121.4 (s, 1.4-difluorobenzene), –149.9 (broad s, *exo* BF_4^-).

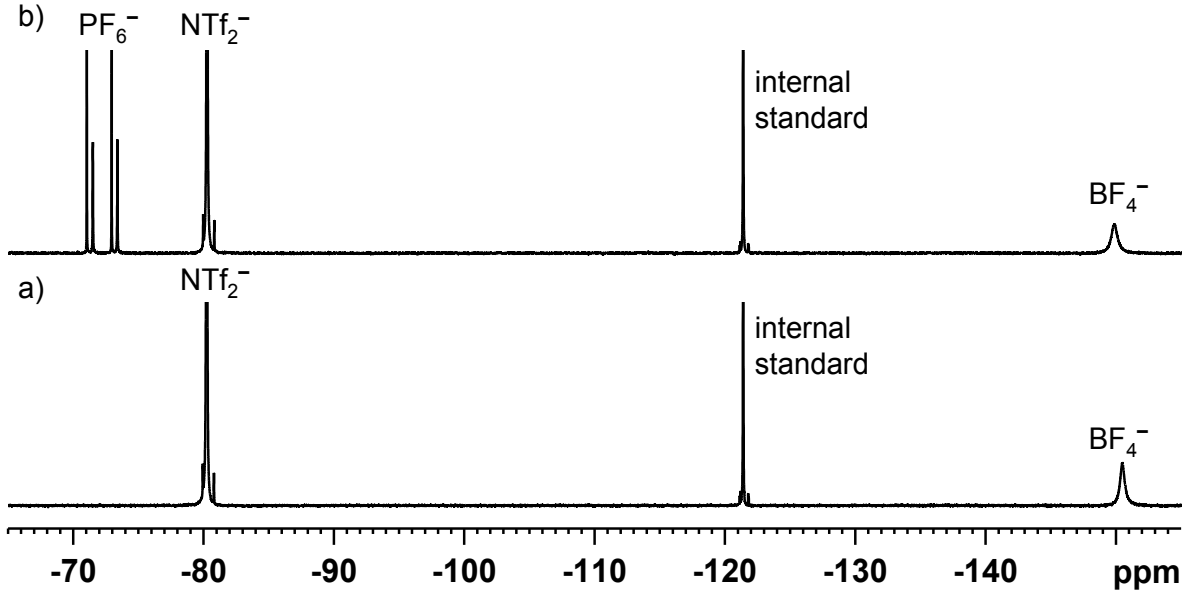

Figure S7: ^{19}F NMR of: a) **BF_4^-⊂1** and b) **PF_6^-⊂1** after displacement of **BF_4^-** (NTf_2^- is the counterion and 1,4-difluorobenzene is the internal standard) (CD_3CN, 400 MHz, 298 K).

Formation of $OTf^-\subset$2 and displacement of OTf^- to form host-guest complex $PF_6^-\subset$2: Into a J-Young NMR tube 3,3′-bipyridine-6,6′-dicarboxaldehyde (2.58 mg, 0.012 mmol, 6 eq.), *p*-chloroaniline (3.19 mg, 0.025 mmol, 12 eq.), and $Fe(CF_3SO_3)_2$ (2.89 mg, 0.0082 mmol, 4 eq.) were dissolved in CD_3CN (0.5 mL). The tube was sealed and the solution was purified of dioxygen by three vacuum/nitrogen fill cycles. The solution was sonicated for 10 minutes and was heated at 323 K for one day.

$OTf^-\subset$2: ^{1}H NMR (400 MHz, 298 K, CD_3CN): δ = 9.42 (s, 2H, imine), 8.72 (d, *J* = 7.84 Hz, 2H, pyridine), 8.31 (d, *J* = 7.84 Hz, 2H, pyridine), 7.31 (d, *J* = 8.18 Hz, 4H, aniline), 7.24 (s, 2H, pyridine), 5.66 (d, *J* = 8.01 Hz, 4H, aniline); ^{19}F NMR (400 MHz, 298 K, CD_3CN): δ = –77.2 (s, 1 *endo* OTf^-), –79.5 (brs, 7 *exo* OTf^-); ESI-MS: *m/z*: 651.6 [**2**+3OTf^-]$^{5+}$, 851.8 [**2**+4OTf^-]$^{4+}$, 1185.6 [**2**+5OTf^-]$^{3+}$.

To the same NMR tube potassium hexafluorophosphate (2.98 mg, 0.016 mmol, 8 eq.) was added.

^{19}F NMR (400 MHz, 298 K, CD_3CN): δ = –72.2 (d, *J* = 717.6 Hz, 1 *endo* PF_6^-), –73.1 (d, *J* = 707.3 Hz, 8 *exo* PF_6^-), –79.5 (s, 8 *exo* OTf^-).

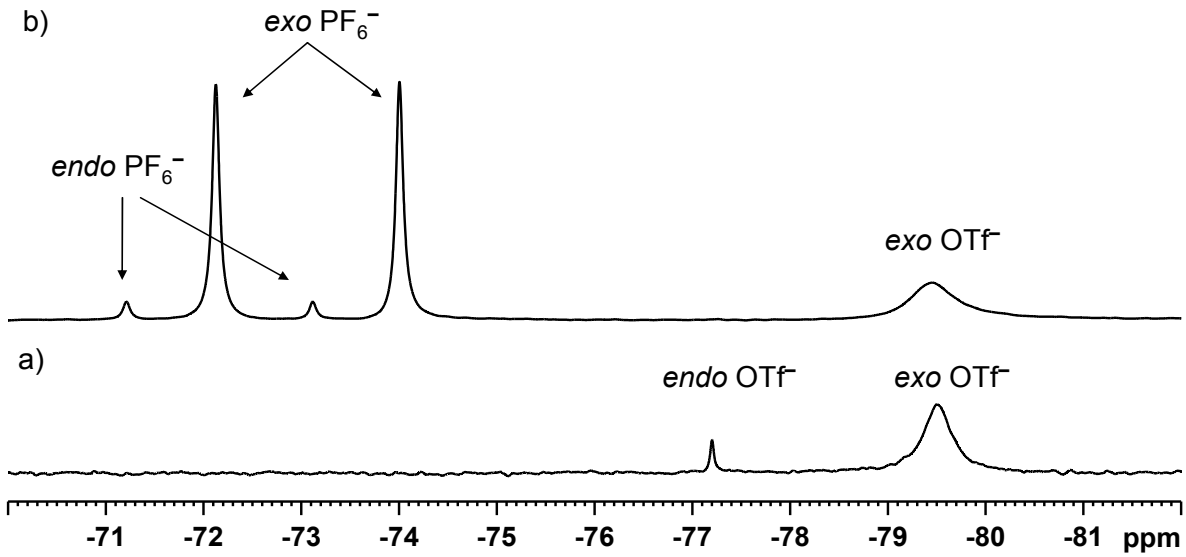

Figure S8: ^{19}F NMR of: a) **$OTf^-\subset$2** and b) **$PF_6^-\subset$2** (CD_3CN, 400 MHz, 298 K).

2. X-ray

Data were collected on a Nonius Kappa FR590 diffractometer employing graphite-monochromated Mo-Kα radiation generated from a sealed tube (0.71073 Å) with ω and ψ scans at 180(2) K.[S3] Data integration and reduction were undertaken with HKL Denzo and Scalepack.[S4] Subsequent computations were carried out using the WinGX-32 graphical user interface.[S5] The structure was solved by direct methods using SIR92 or SIR97.[S6-7] Multi-scan empirical absorption corrections, when applied, were applied to the data set using the program SORTAV.[S8] Data were refined and extended with SHELXL-97.[S9] In general non-hydrogen atoms with occupancy of greater than 0.5 were refined anisotropically and hydrogen atoms were refined using a riding model. Specific details and data for each structure follow.

[OTf$^-$⊂**1**]·7NTf$_2$·5MeCN

Formula $C_{169}H_{123}F_{45}Fe_4N_{36}O_{31}S_{10}$, M 4553.03, monoclinic, space group $C2$(#5), a 26.876(5), b 38.443(8), c 22.391(5) Å, β 94.44(3), V 23064(8) Å^3, D_c 1.311 g cm^{-3}, Z 4, crystal size 0.50 × 0.35 × 0.10 mm, colour purple, habit plate, temperature 180(2) K, λ(MoKα) 0.71073 Å, μ(MoKα) 0.439 mm^{-1}, T(SORTAV)$_{min,max}$ 0.614, 0.952, 2θ_{max} 50.06, *hkl* range –31 31, –42 45, –26 26, N 48613, N_{ind} 28751(R_{merge} 0.0704), N_{obs} 16997(I > 2σ(I)), N_{var} 1048, residuals $R1(F)$ 0.1069, $wR2(F^2)$ 0.3103, GoF(all) 1.062, $\Delta\rho_{min,max}$ –0.644, 1.101 e$^-$ Å^{-3}.

Specific details:

Crystals were grown by diffusion of diisopropyl ether into the acetonitrile solution of [OTf$^-$⊂**1**]·7NTf$_2$ that was obtained by titration of one equivalent of triflate into the acetonitrile solution of **1**(NTf$_2$)$_8$ (see section S4 below). The crystals were diffracted poorly and rapidly suffered solvent loss. Despite rapid handling times and a low temperature collection no reflection data were observed at better than 1.0 Å resolution. In addition the crystals appeared to decay further during data collection resulting in lower than ideal completeness. Due to the low quality of the data numerous rigid body restraints (AFIX 66) were required in the phenyl and pyridyl rings and each of the rings that had such a restraint applied were refined with identical thermal parameters resulting in a large discrepancy in the thermal parameters of adjacent atoms.

Nevertheless, the quality of the data is more than sufficient for establishing the connectivity of the structure. The structure has a pseudo higher symmetry, but is in fact a racemic twin. The encapsulated anions are disordered over two positions across a special position and were modelled with rigid body restraints. The triflimide anions within the lattice were significantly disordered and two of them could be successfully modelled. While the heavy atoms of the remaining anions could be located in the difference Fourier map the remainder of the anions could not and despite numerous attempts at modelling, including with multiple rigid bodies no satisfactory model for the electron-density associated with them could be found. Therefore the SQUEEZE function of PLATON[S10] was employed to remove the contribution of the electron density associated with these anions from the model, which resulted in far more satisfactory residuals reducing the R-factor from 20 % to 10.69 %.

[MeCN⊂**1**]·8NTf$_2$·MeCN

Formula $C_{254}H_{114}F_{24}Fe_4N_{34}O_{32}S_{16}$, M 5346.15, monoclinic, space group $P2_1/c$(#14), a 35.2292(14), b 20.7057(7), c 34.2007(10) Å, β 104.740(2), V 24126.5(14) Å^3, D_c 1.472 g cm^{-3}, Z 4, crystal size 0.46 × 0.35 × 0.02 mm, purple plate, temperature 180(2) K, μ(MoKα) 0.471 mm^{-1}, T(SORTAV)$_{min,max}$ 0.631, 1.145, $2\theta_{max}$ 37.66, *hkl* range –16 31, –18 18, –29 29, N 15280, N_{ind} 10563(R_{merge} 0.0969), N_{obs} 6332(I > 2σ(I)), N_{var} 533, residuals* $R1(F)$ 0.1134, $wR2(F^2)$ 0.3177, GoF(all) 1.069, $\Delta\rho_{min,max}$ –0.492, 0.576 e$^-$ Å^{-3}.

Specific details:

Crystals were grown by the slow diffusion of toluene into an acetonitrile solution of **1**·8NTf$_2$. The crystals were small and poor diffractors and rapidly suffered solvent loss. Despite rapid handling times and a low temperature collection no reflection data were observed at better than 1.2 Å resolution. In addition the crystals appeared to decay further during data collection resulting in lower than ideal completeness and redundancy. Due to the low quality of the data, only the iron atoms were refined anisotropically. A number of rigid body restraints were required on the phenyl rings of the systems to facilitate realistic modelling. Nevertheless, the quality of

the data is more than sufficient for establishing the connectivity of the structure. The anions within the lattice were significantly disordered and despite numerous attempts at modelling, including with multiple rigid bodies no satisfactory model for the electron-density associated with them could be found. Therefore the SQUEEZE function of PLATON[S10] was employed to remove the contribution of the electron density associated with the anions from the model, which resulted in far more satisfactory residuals.

3. Volume Calculations

In order to determine the size of the inner cavity of **1** VOIDOO calculations based on the crystal structure of **1** were performed.[S11] A virtual probe with a radius of 1.4 Å (default, water-sized) was employed, and the following parameters were changed from their default settings:

Maximum number of volume-refinement cycles:	30
Minimum size of secondary grid:	3
Grid for plot files:	0.1
Primary grid spacing:	0.1
Plot grid spacing:	0.1

Due to the large pore size of **1**, six benzene molecules were placed over the pores to prevent the probe from "falling out" of the inner sphere. They were placed in such a way that the van der Waals radii of their atoms touched the outermost edge of the van der Waals radii of the atoms of **1** lining the pores. The cavity was visualised as a green mesh inside the crystal structure of **1** (see Figure S9). The same mesh was overlaid with space-filling models of 4 anions (tetrafluoroborate, hexafluorophosphate, triflate and triflimide) for size comparison. Using SPARTAN,[S12] the molecular volumes of these anions were calculated as follows:

BF_4^-:	59 Å^3
PF_6^-:	75 Å^3
OTf^-:	86 Å^3
NTf_2^-:	157 Å^3

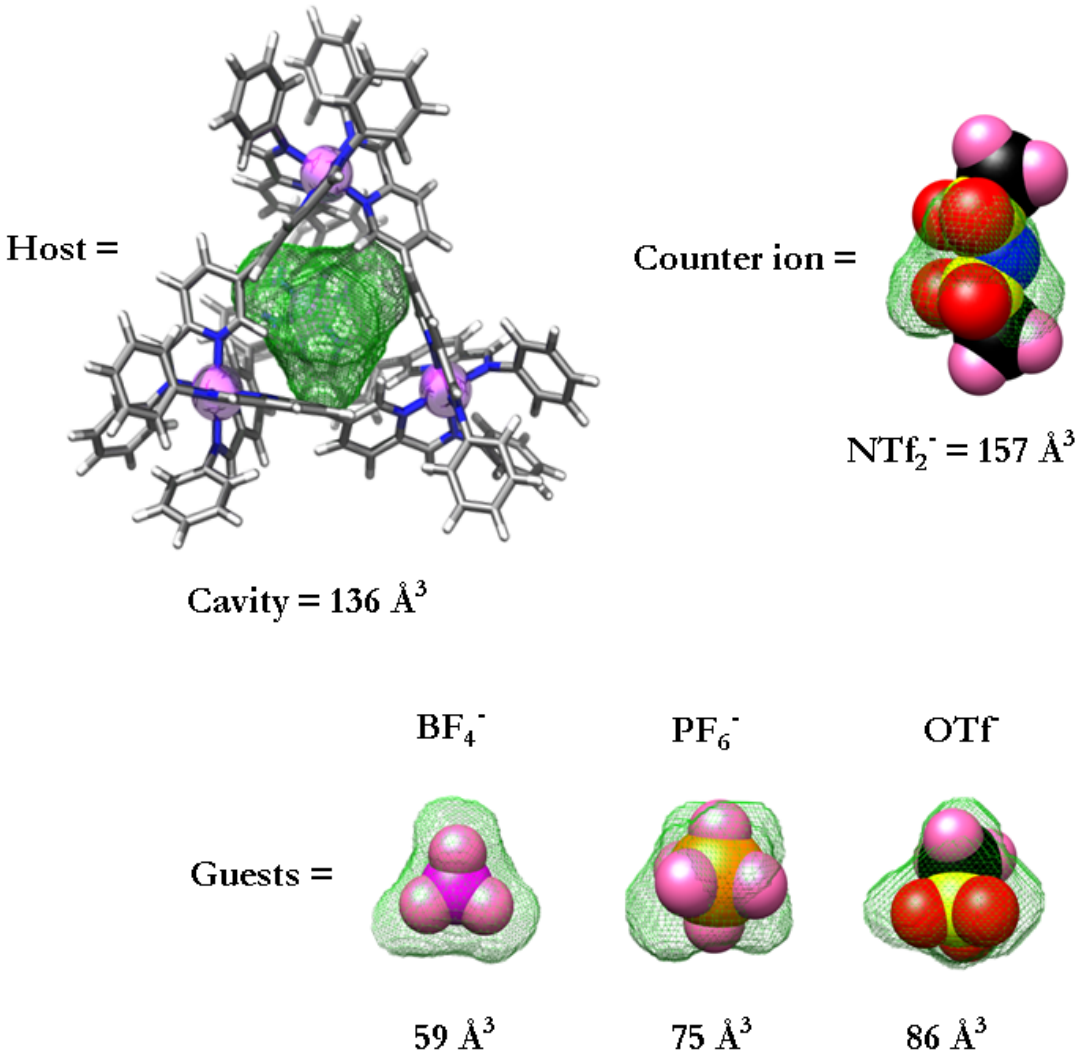

Figure S9: VOIDOO-calculated void space as shown (green mesh) within the crystal structure of **1**, as well as overlay of the same void space with 4 anions for size comparison.

4. K_a Determination

4.1. Derivation of the expression of the fraction of occupied host as a function of total guest concentration

Consider the equilibrium between a host *H* and a guest *G* that can form host-guest complex *HG*:

$$H + G \rightleftharpoons HG \quad \text{(S1)}$$

The equilibrium (binding) constant *K* for this equilibrium is defined as:

$$K = \frac{[HG]}{[H][G]} \quad \text{(S2)}$$

From S2 it follows that the equilibrium concentration of host-guest complex, [*HG*], can be expressed as:

$$[HG] = K\,[H][G] \quad \text{(S3)}$$

Furthermore we can write the mass balance for the total guest ($[G]_0$) and total host ($[H]_0$) concentration:

$$[G]_0 = [G] + [HG] = [G] + K[H][G] \quad \text{(S4)}$$

$$[H]_0 = [H] + [HG] = [H] + K[H][G] = [H]\times(1 + K[G]) \quad \text{(S5)}$$

Let us now define the fraction of occupied host as:

$$y = \frac{[HG]}{[H]_0} = \frac{K[H][G]}{[H]\times(1 + K[G])} = \frac{K[G]}{1 + K[G]} \quad \text{(S6)}$$

Equation S6 allows one to determine the binding constant *K* if the fraction of occupied host is known as a function of **free guest concentration at equilibrium** ([*G*]). Below we show that [*G*] can be expressed in terms of $[G]_0$, $[H]_0$ and *K*.

From S4 and S3 it follows that the free guest concentration at equilibrium is equal to:

$$[G] = [G]_0 - [HG] = [G]_0 - K[H][G] \quad \text{(S7)}$$

From S5 and S6 it follows that the free host concentration at equilibrium is equal to:

$$[H] = (1 - y)[H]_0 \quad \text{(S8)}$$

Combining S7 and S8 yields:

$$[G] = [G]_0 - K(1 - y)[H]_0[G] \quad \text{(S9)}$$

Rearranging S9 gives:

$$(1 + K(1 - y)[H]_0) \times [G] = [G]_0 \quad \text{(S10)}$$

From S10 it follows that the free guest concentration at equilibrium is equal to:

$$[G] = \frac{[G]_0}{1 + K(1 - y)[H]_0} \quad \text{(S11)}$$

Rearranging S6 gives:

$$y + yK[G] = K[G] \quad \text{(S12)}$$

Inserting S11 in S12 yields:

$$y + yK\left(\frac{[G]_0}{1 + K(1 - y)[H]_0}\right) = K\left(\frac{[G]_0}{1 + K(1 - y)[H]_0}\right) \quad \text{(S13)}$$

Rearranging S13 yields:

$$y(1 + K(1 - y)[H]_0) + yK[G]_0 = K[G]_0 \quad \text{(S14)}$$

Rearranging S4 yields:

$$y(1 + K[H]_0 - Ky[H]_0) + yK[G]_0 - K[G]_0 = 0 \quad \text{(S15)}$$

Rearranging S15 yields:

$$-K[H]_0y^2 + (1 + K([H]_0 + [G]_0))y - K[G]_0 = 0 \quad \text{(S16)}$$

Finally, we can rewrite S16 to:

$$K[H]_0y^2 - (1 + K([H]_0 + [G]_0))y + K[G]_0 = 0 \quad \text{(S17)}$$

Equation S17 is a quadratic equation in y, which can be solved yielding two roots:

$$y = \frac{[1 + K([H]_0 + [G]_0)] \pm \sqrt{[1 + K([H]_0 + [G]_0)]^2 - 4K^2[H]_0[G]_0}}{2K[H]_0}$$

(S18)

From the two roots of S18, it was found that the physically meaningful root is given by:

$$y = \frac{[1 + K([H]_0 + [G]_0)] - \sqrt{[1 + K([H]_0 + [G]_0)]^2 - 4K^2[H]_0[G]_0}}{2K[H]_0}$$

(S19)

Equation S19 was used to fit the binding data, using Origin. To this end, S19 was adapted to give:

Y=Y0+DY*((Ka*(P+x)+1)–SQRT(((Ka*(P+x)+1)^2)–4*Ka*Ka*P*x))/(2*Ka*P) (S20)

Y	Measured Chemical shift
Y0	Chemical shift of empty host solution
DY	Maximal change in chemical shift: the difference in chemical shift of a fully occupied host and an empty host
Ka	Binding constant
P	Total host concentration
x	Total guest concentration

4.2. Derivation of the equations for competitive binding studies

Consider the equilibrium between a host H and a guest G_1 that can form host-guest complex HG_1:

$$H + G_1 \rightleftharpoons HG_1 \quad \text{(S21)}$$

The equilibrium (binding) constant K_1 for this equilibrium is defined as:

$$K_1 = \frac{[HG_1]}{[H][G_1]} \quad \text{(S22)}$$

Similarly for Guest G_2 we can derive:

$$H + G_2 \rightleftharpoons HG_2 \quad \text{(S23)}$$

$$K_2 = \frac{[HG_2]}{[H][G_2]} \quad \text{(S24)}$$

The mass balances for guest G_1, guest G_2 and host are given by:

$$[G_1]_0 = [G_1] + [HG_1] \quad \text{(S25)}$$

$$[G_2]_0 = [G_2] + [HG_2] \quad \text{(S26)}$$

$$[H]_0 = [H] + [HG_1] + [HG_2] \quad \text{(S27)}$$

Combining S22 and S24 yields:

$$\frac{K_2}{K_1} = \frac{[HG_2]}{[G_2]} \cdot \frac{[G_1]}{[HG_1]} \quad \text{(S28)}$$

For simplicity let us define the following concentrations:

$[H]_0 = p$

$[G_2]_0 = x$

$[HG_2] = y$

$[G_1]_0 = r$

Furthermore, we will assume that: [H] ≈ 0. This means that S27 becomes:

$$[H]_0 = [HG_1] + [HG_2] \quad \text{(S29)}$$

Rearranging S29 and inserting the new variables yields:

$$[HG_1] = [H]_0 - [HG_2] = p - y \quad \text{(S30)}$$

Similarly, by rearranging S26 we find:

$$[G_2] = [G_2]_0 - [HG_2] = x - y \quad \text{(S31)}$$

While rearranging S25 yields:

$$[G_1] = [G_1]_0 - [HG_1] = r - (p - y) \quad \text{(S32)}$$

Inserting S30, S31 and S32 in S28 gives:

$$\frac{K_2}{K_1} = B = \frac{[HG_2]}{[G_2]} \cdot \frac{[G_1]}{[HG_1]} = \frac{y}{x-y} \cdot \frac{r-(p-y)}{p-y} = \frac{y^2 + (r-p)y}{y^2 - (x+p)y + px} \quad \text{(S33)}$$

Here we have defined B as the ratio of the two binding constants.

Rearranging S33 gives:

$$By^2 - B(x+p)y + pxB = y^2 + (r-p)y \quad \text{(S34)}$$

Rearranging S34 gives:

$$(B-1)y^2 - [B(x+p) + (r-p)]y + pxB = 0 \qquad \text{(S35)}$$

Equation S35 is a quadratic equation in y, which can be solved yielding two roots:

$$y = \frac{[B(x+p) + (r-p)] \pm \sqrt{[B(x+p) + (r-p)]^2 - 4(B-1)Bxp}}{2(B-1)} \qquad \text{(S36)}$$

From the two roots of S36, it was found that the physically meaningful root is given by:

$$y = \frac{[B(x+p) + (r-p)] - \sqrt{[B(x+p) + (r-p)]^2 - 4(B-1)Bxp}}{2(B-1)} \qquad \text{(S37)}$$

If we now replace the variables by their corresponding concentration, we get:

$$[HG_2] = \frac{\left[\frac{K_2}{K_1}([G_2]_0 + [H]_0) + ([G_1]_0 - [H]_0)\right] - \sqrt{\left[\frac{K_2}{K_1}([G_2]_0 + [H]_0) + ([G_1]_0 - [H]_0)\right]^2 - 4\left(\frac{K_2}{K_1} - 1\right)\frac{K_2}{K_1}[G_2]_0[H]_0}}{2\left(\frac{K_2}{K_1} - 1\right)} \qquad \text{(S38)}$$

To fit the binding data, equation S37 was used. To this end, S37 was adapted to the following equation that was used in Origin to fit the data:

Y=((B*(x+P)+(R–P))–SQRT(((B*(x+P)+(R–P))^2)–4*(B–1)*(B*x*P)))/(2*(B–1)) (S39)

Y Concentration of Host-Guest2 complex = $[HG_2]$

B Ratio of the two binding constants = K_2 / K_1

P Total host concentration = $[H]_0$

R Total Guest1 concentration = $[G_1]_0$

x Total Guest2 concentration = $[G_2]_0$

4.3. NMR Titrations

^{1}H NMR titration conditions for determining K_a values for 1-to-1 binding of BF_4^- inside Host 1:

$[\mathbf{1}]_0 = 7.8\times10^{-4}$ M, $[BF_4^-] = 1.0\times10^{-2}$ M; the concentration of host **1** was kept constant throughout the titration experiment and small aliquots of guest solution were titrated in a J-Young NMR tube before each spectrum was acquired.

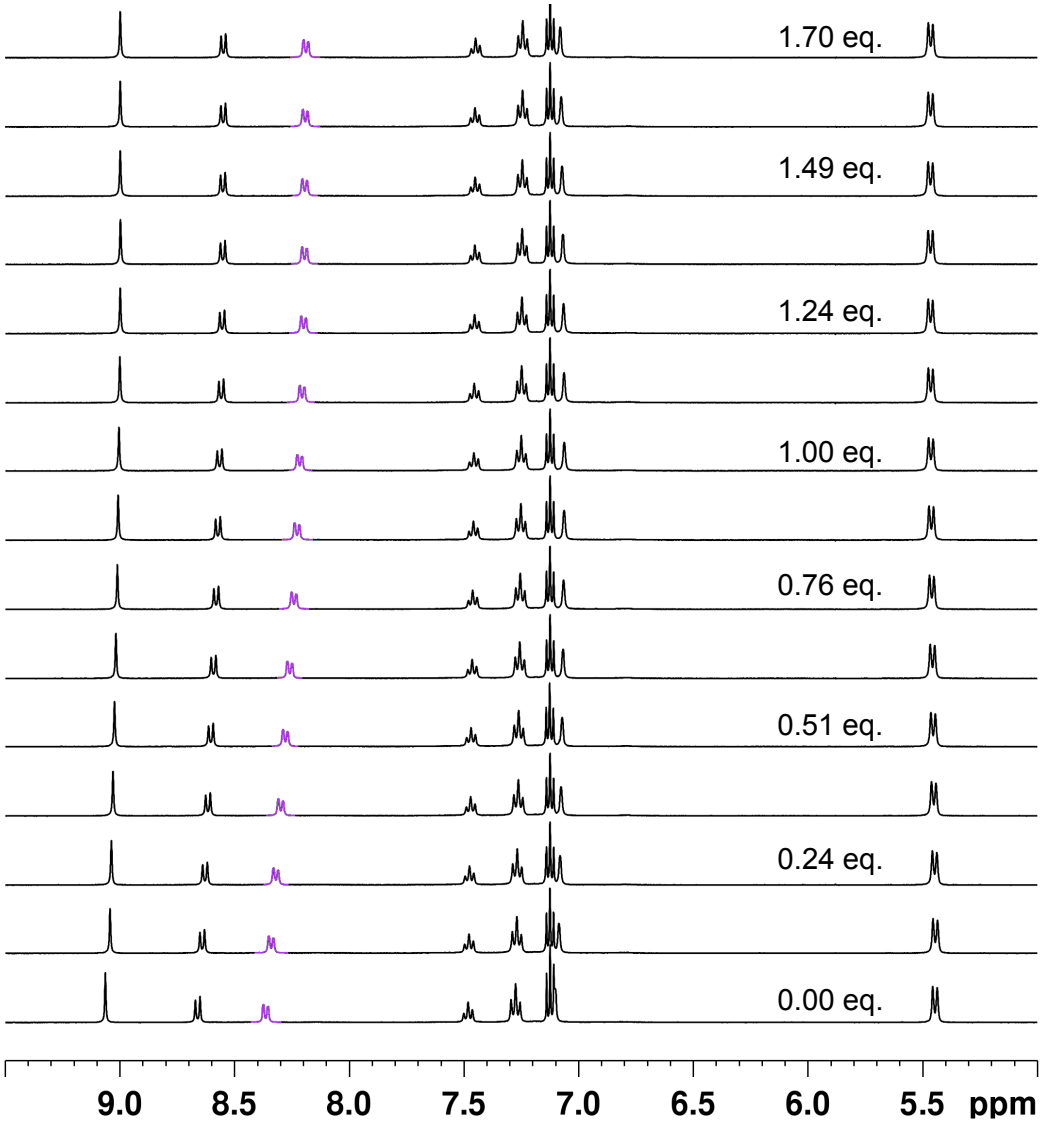

Figure S10: ^{1}H NMR stack plot of the aromatic region for the titration of BF_4^- into a solution of **1**. The fitting in Figure S11 is based on the chemical shift of the doublet in purple (CD_3CN, 400 MHz, 298 K).

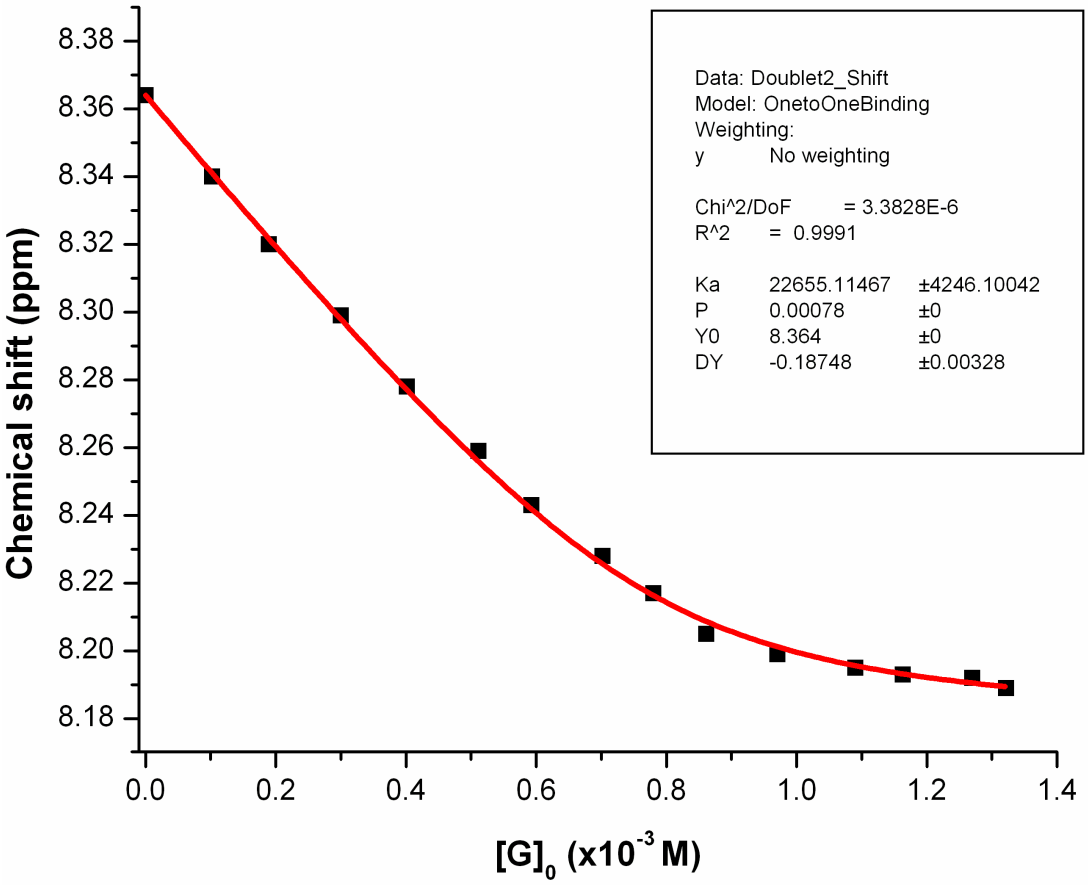

Figure S11: Data fitting for the titration of fast exchanging BF_4^- guest into a solution of **1**. A binding constant of $2.3\times10^4 \pm 4.2\times10^3$ M^{-1} was determined for $BF_4^-\subset$**1**.

^{1}H NMR titration conditions for determining K_a values for 1-to-1 binding of OTf^- inside Host 1:

$[\mathbf{1}]_0 = 7.8\times10^{-4}$ M, $[OTf^-] = 1.0\times10^{-2}$ M; the concentration of host **1** was kept constant throughout the titration experiment and small aliquots of guest solution were titrated in a J-Young NMR tube before each spectrum was acquired.

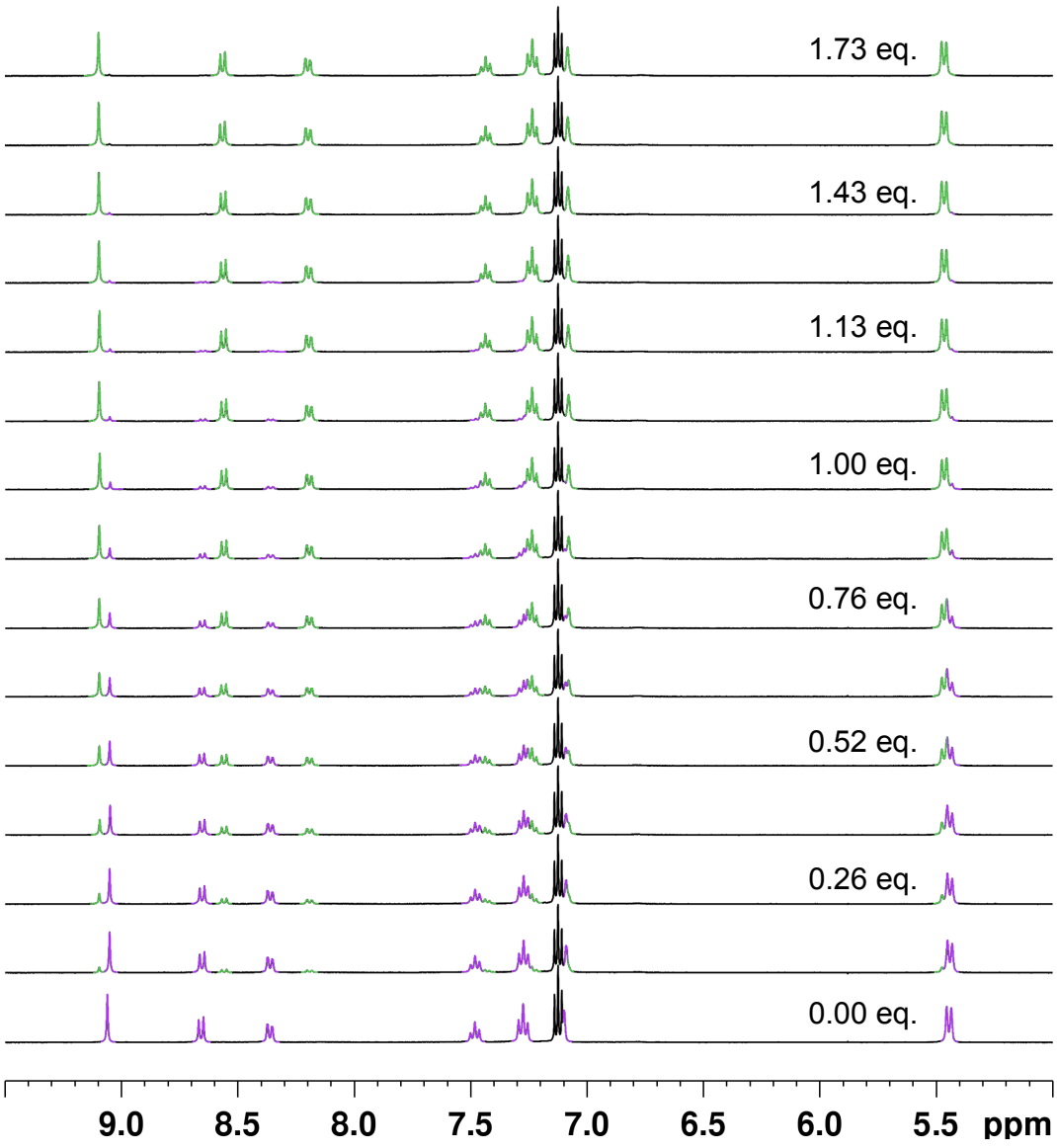

Figure S12: ^{1}H NMR stack plot of the aromatic region for the titration of OTf^- into a solution of **1**. Signals in purple correspond to empty host **1** and signals in green to $OTf^-\subset$**1** (CD_3CN, 400 MHz, 298 K).

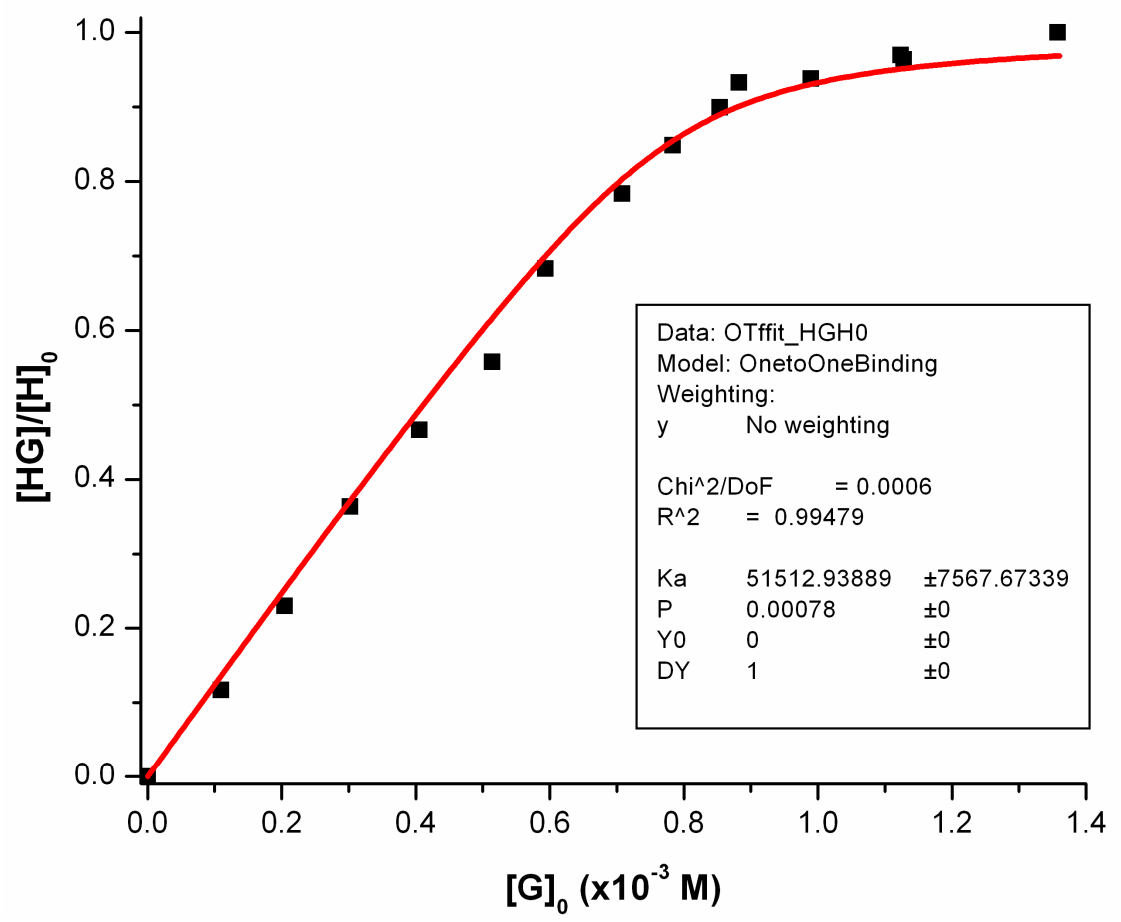

Figure S13: Data fitting for the titration of the slow exchanging OTf^- guest into a solution of **1**.

A binding constant of $5.2\times10^4 \pm 7.6\times10^3$ M^{-1} was determined for $OTf^-\subset$**1**.

^{1}H NMR titration conditions for determining K_a values for 1-to-1 binding of PF_6^- inside Host 1:

$[\mathbf{1}]_0 = 7.8\times10^{-4}$ M, $[OTf^-] = 7.8\times10^{-4}$ M, $[PF_6^-] = 1.0\times10^{-2}$ M; the concentrations of host **1** and OTf^- were kept constant throughout the titration experiment and small aliquots of guest solution were titrated in a J-Young NMR tube before each spectrum was acquired.

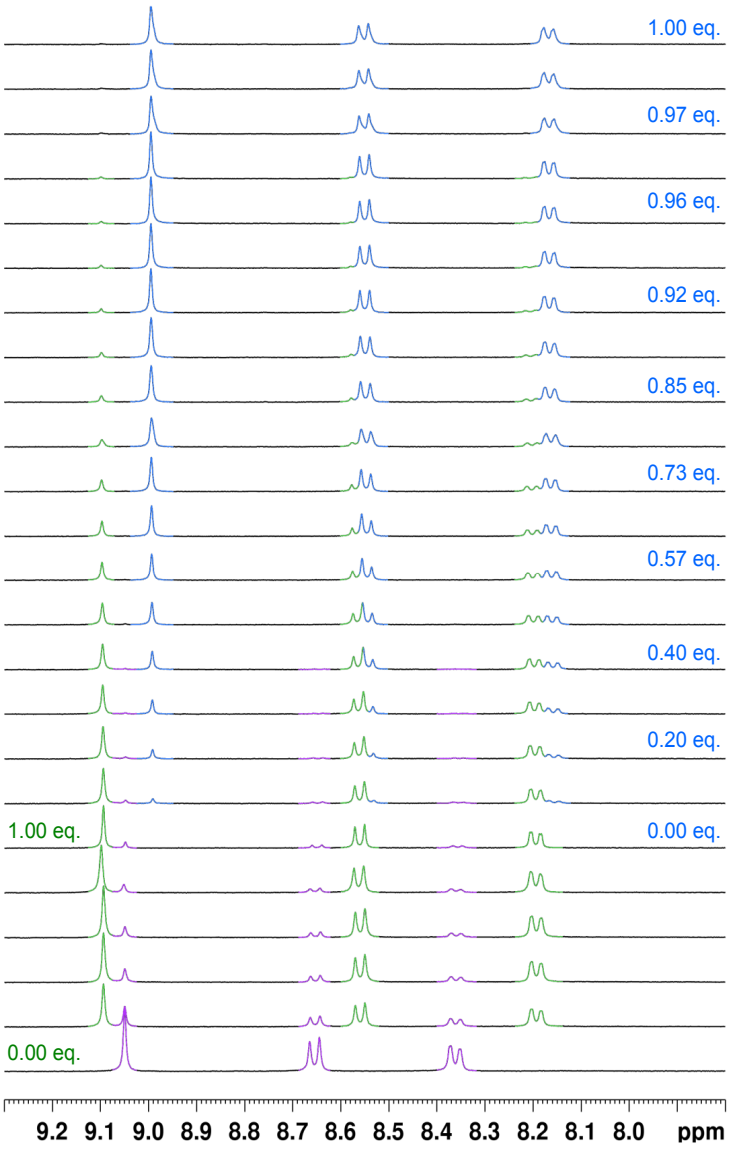

Figure S14: ^{1}H NMR stack plot of part of the aromatic region for the competitive binding titration experiment of PF_6^- into a solution of $OTf^-\subset$**1**. Signals in purple correspond to empty host **1**, signals in green to $OTf^-\subset$**1** and signals in blue to $PF_6^-\subset$**1** (CD_3CN, 400 MHz, 298 K).

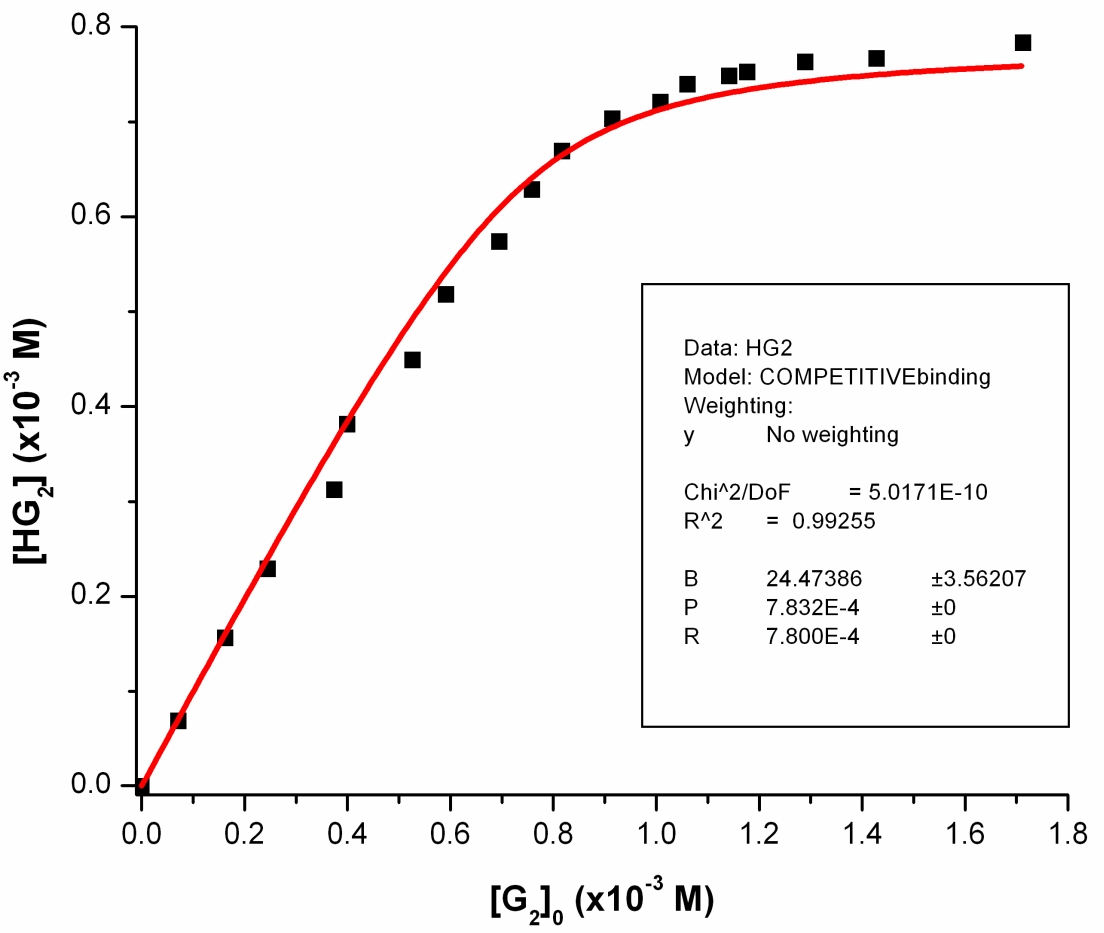

Figure S15: Data fitting for the competitive binding experiment between $OTf^-\subset$**1** and $PF_6^-\subset$**1**. A value of 24.4 ± 3.6 was determined for B (= K_2 / K_1), which means that the binding constant for $PF_6^-\subset$**1** is equal to $1.3\times10^6 \pm 2.6\times10^5$ M^{-1}.

5. Determination of the number of cages that differ in mass

Cages that are different mass will differ in the number of *p*-bromoaniline, and *p*-chloroaniline and *p*-iodoaniline residues incorporated into the cage's exterior. Hence, we need to calculate the number of possibilities to fill the available 12 'positions' on the cage with a unique combination of 3 candidates (*i.e.* the 3 anilines). For convenience, we will call these 3 candidates A, B and C. Consider the individual cases for a given number of A candidates. There are 13 such cases: N_A = 0, 1, 2, …., 10, 11 or 12 A-filled positions.

N_A = 0

If there are no positions filled by A, then all remaining 12 positions are filled by B and/or C candidates. There are 13 possibilities to arrange B and C candidates over 12 positions. That is, the 12 positions can be filled with 0, 1, 2, …., 10, 11 or 12 B candidates (the remaining positions are then automatically taken by C candidates.

N_A = 1

There are now 11 remaining positions for B and or C. Following the reasoning for N_A = 0, there are in this case 12 possibilities to arrange the B and C candidates over the 11 remaining positions.

N_A = 2

There are now 10 remaining positions for B and or C. Following the reasoning for N_A = 0 and N_A = 1, there are in this case 11 possibilities to arrange the B and C candidates over the 10 remaining positions.

By similar reasoning we can compose the following table, which shows a total of **91** possible combinations for 12 positions that can be filled with a combination of 3 candidates.

Table S1: Number of different combinations for a given number of A candidates.

N_A	$N_B + N_C$	**No. of possibilities to arrange B and C over the remaining vacant positions**
0	12	13
1	11	12
2	10	11
3	9	10
4	8	9
5	7	8
6	6	7
7	5	6
8	4	5
9	3	4
10	2	3
11	1	2
12	0	1
Total		**91**

Note: From the table above it can be concluded that in the case of 3 candidates and N vacancies, the total number of possibilities, P, is given by:

$$P = 1 + 2 + 3 + \ldots + N + N+1 = 0.5\times[(N+1)^2 + (N+1)] = 0.5\times[(N)^2 + 3N + 2)] \quad \text{(S40)}$$

6. References

S1. A. Angeloff, J.-C. Daran, J. Bernadou and B. Meunier, *European Journal of Inorganic Chemistry*, 2000, 1985-1996.
S2. A.-J. Attias, C. Cavalli, B. Bloch, N. Guillou and C. Noël, *Chem. Mater.*, 1999, **11**, 2057-2068.
S3. N. BV, *COLLECT*, (1998) Nonius BV, Delft, The Netherlands.
S4. Z. Otwinowski and W. Minor, *Methods in Enzymology*, 1997, **276**, 307-326.
S5. L. Farrugia, *J. Appl. Cryst.*, 1999, **32**, 837-838.
S6. A. Altomare, M. C. Burla, M. Camalli, G. Cascarano, C. Giacovazzo, A. Guagliardi and G. Polidori, *J. Appl. Cryst.*, 1994, **27**, 435.
S7. A. Altomare, M. C. Burla, M. Camalli, G. L. Cascarano, C. Giocavazzo, A. Gaugliardi, G. C. Moliterni, G. Polidori and S. Spagna, *J. Appl. Crystallogr.*, 1999, **32**, 115.
S8. R. H. Blessing, *Acta Cryst.*, 1995, **A51**, 33-38.
S9. G. M. Sheldrick, *SHELXL-97: Programs for Crystal Structure Analysis, University of Göttingen, Germany*, 1997.
S10. A. L. Spek, *Acta Crystallogr.*, 1990, **A46**, C34.
S11. G. J. Kleywegt and T. A. Jones, *Acta. Cryst.*, 1994, **D50**, 178-185.
S12. I. Wavefunction, *SPARTAN '04 for windows*, (2004) Wavefunction, Inc., Irvine (CA), USA.